AD-A235 646

(2)

Proceedings of the Conference on

Recent Advances in Active Control of Sound and Vibration

DTIC

General Chairman: C. R. Fuller
Technical Chairman: R. A. Burdisso
Program Editors: C. A. Rogers, C. R. Fuller

Virginia Polytechnic Institute
and State University
Blacksburg, Virginia

15–17 April, 1991

Sponsored by:
NASA Langley Research Center
Office of Naval Research
U.S. Army Aerostructures Directorate

A-1 20

TECHNOMIC PUBLISHING CO., INC.
LANCASTER · BASEL

91 5 09 033

REPORT DOCUMENTATION PAGE

Form Approved
OMB No. 0704-0188

1. AGENCY USE ONLY *(Leave blank)*

2. REPORT DATE
1991

3. REPORT TYPE AND DATES COVERED
Article from Proceedings

4. TITLE AND SUBTITLE Article Title:
Stabilization of a Digitally Controlled Active-Isolation System

5. FUNDING NUMBERS
P.E. #61153N
Task #RR011-08-42
W.U. #59-0582-0-0
Assession #DNA580-030

6. AUTHOR(S) S. E. Forsythe, Code 5930
M. D. McCollum, Code 5976
A. D. McCleary, Code 5977

7. PERFORMING ORGANIZATION NAME(S) AND ADDRESS(ES)
Underwater Sound Reference Detachment
Naval Research Laboratory
P.O. Box 568337
Orlando, FL 32856-8337

8. PERFORMING ORGANIZATION REPORT NUMBER

9. SPONSORING/MONITORING AGENCY NAME(S) AND ADDRESS(ES)
Office of Naval Research via Naval Research Laboratory

10. SPONSORING/MONITORING AGENCY REPORT NUMBER

11. SUPPLEMENTARY NOTES
Proceedings Title: Conference on Recent Advances in Active Control of Sound and Vibration
Held 15-17 April 1991 in Blacksburg, VA

12a. DISTRIBUTION/AVAILABILITY STATEMENT
Approved for public release; distribution unlimited

12b. DISTRIBUTION CODE

13. ABSTRACT *(Maximum 200 words)*
Digital control techniques have proved beneficial in many control applications because they are flexible and lend themselves to adaptive implementations. However, in control systems that require feedback rather than feedforward as the control mechanism, the advantages of digital control are offset by the difficulty of designing stable controllers. The time lag introduced by the sampling process itself is compounded by the time lag introduced by anti-aliasing filters. These lags, in conjunction with low sampling rates, make an otherwise stable system subject to instability if high open-loop gains are required. This paper will focus on a technique for adding an empirical model of the system under control to the control loop as a means of stabilizing the system.

14. SUBJECT TERMS
Feeback Control, Stabilization, Adaptive Control
Digital Control, Channel Modeling

15. NUMBER OF PAGES
19

16. PRICE CODE

17. SECURITY CLASSIFICATION OF REPORT	18. SECURITY CLASSIFICATION OF THIS PAGE	19. SECURITY CLASSIFICATION OF ABSTRACT	20. LIMITATION OF ABSTRACT
Unclassified	Unclassified	SAR	SAR

Recent Advances in Active Control of Sound and Vibration
a TECHNOMIC publication

Published in the Western Hemisphere by
Technomic Publishing Company, Inc.
851 New Holland Avenue
Box 3535
Lancaster, Pennsylvania 17604 U.S.A.

Distributed in the Rest of the World by
Technomic Publishing AG

Printed in the United States of America

10 9 8 7 6 5 4 3 2 1

Main entry under title:
Recent Advances in Active Control of Sound and Vibration

A Technomic Publishing Company book
Bibliography: p.

Library of Congress Card No. 91-65229
ISBN No. 87762-839-4

Contents

STABILIZATION OF A DIGITALLY CONTROLLED ACTIVE-ISOLATION SYSTEM

S. E. Forsythe,[1] M. D. McCollum,[1] A. D. McCleary[1]

ABSTRACT

Digital control techniques have proved beneficial in many control applications because they are flexible and they lend themselves to adaptive implementations. However, in control systems that require feedback, rather than feedforward, as the control mechanism the advantages of digital control are offset by the difficulty of designing stable controllers. The time lag introduced by the sampling process itself is compounded by the time lag introduced by anti-aliasing filters. These lags, in conjunction with low sampling rates, make an otherwise stable system subject to instability if high open-loop gains are required. This paper will focus on a technique for adding an empirical model of the system under control to the control loop as a means of stabilizing the system.

INTRODUCTION

The objective of this effort is to create an active planar element that has one face held to zero motion in the presence of vibration at the other face. The active element consists of two flat piezoelectric elements bonded together: an actuator which is placed next to the vibrating face and a sensor which is used to measure motion of the other face. The actuator is used to counter motion of the vibrating surface and the sensor is used to measure residual motion of the controlled surface. The planar element has resonances but below the first resonance it can be assumed that the transfer of electrical and mechanical energy is primarily through thickness modes so that voltages applied and read are truly representative of the normal motion of the surface. An independent accelerometer is used to verify the performance of the surface element.

The strong coupling from the actuator to the sensor makes control of the system different from many active noise cancellation applications where the two are physically separated and there is little or no feedback from the compensator to the sensor.

This paper is confined to the control theory aspects of the system outlined above. The mechanical aspects of the problem are discussed in a companion paper [1].

This paper is organized into four sections: description of the control problem to be solved and a derivation of the control equation; details of the derivation of the model and control transfer functions; a presentation

[1]Naval Research Laboratory, Underwater Sound Reference Detachment, PO Box 568337, Orlando, FL 32856 8337, USA

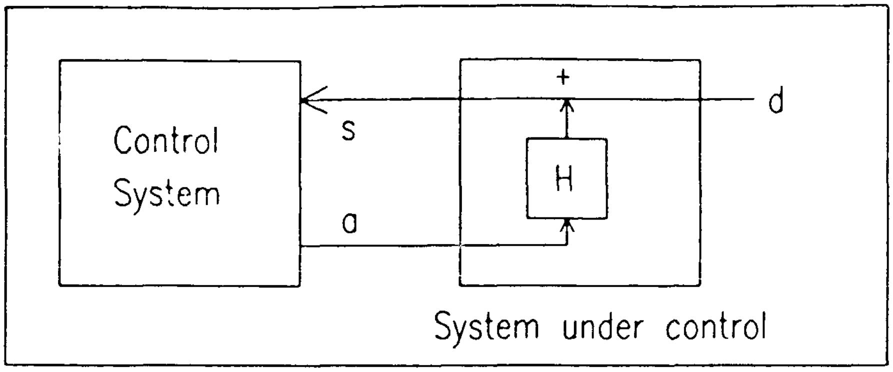

Figure 1 - overview of controller and controlled system

of experimental setup and actual real-time cancellation results; and a discussion of future work on this technique.

DESCRIPTION OF THE PROBLEM AND DERIVATION OF THE CONTROL EQUATION

Figure 1 is an illustration of the system we wish to control and the attached controller. At this point, the controller is specified as a black box so that we can focus on the mechanical/electrical system under control. A disturbance **d** is presented to the system. Without loss of generality, it can be assumed that a copy of **d** is available to the sensor input **s** of the control system (any system transfer function from **d** to **s** can be lumped with the source). Further, the control system can influence the behavior of the system at the summing point by applying an actuator control signal **a** to the system. The actuator's effect is felt at the summing point after passing through a loop transfer function, **H**. In our apparatus, the summing point represents the motion of the top surface. It is this motion and the corresponding signal **s** that we wish to drive to zero by application of the appropriate control signal **a**.

In terms of classical control theory, the controller in the loop can be represented by the transfer function **G** (which is to be determined) that converts the sensor's reading into a control output to the actuator. The equation relating **s** to **d** is then

$$s = \frac{d}{1 - GH}. \tag{1}$$

Note the sign. Both signals add at the junction. Classical control theory says that **s** can be driven toward zero over some frequency range by choosing **G** to make the product **GH** large over that range. However, this leads to the potential instability problems mentioned above.

Fig. 2 shows the "interior" of the controller: a model **M** of **H** is introduced in a parallel negative feedback loop implemented within the control system itself. This model **M** is designed to reproduce as closely as possible the response of **H**. Note that **M** can be implemented in any fashion (analog, digital, etc.).

The response of the compensated system at s1 (the input to the control box, G) is

$$s1 = \frac{d}{1 + G(M - H)}. \tag{2}$$

Note the sign of **M** in the denominator; the output of **M** is subtracted at the summing point. When in the loop, the model reduces the effect of the actuator **a** on the input to **G**. In fact, if the model is perfect (**M**=**H**) then **s1** = **d** and the input to **G** is only a replica of the original disturbance signal, uncontaminated by the effects of the actuator. This effectively opens the loop. Further, with the model in the loop, the new expression for **s** is

$$s = \frac{d(1 + GM)}{1 + G(M - H)}. \tag{3}$$

In the best possible case, if **M** ≡ **H** and **GM** ≡ -1 (**G** ≡ -1/**M**), by construction, then **s** is identically zero independent of **d**, the disturbance. This is equivalent to perfect broadband cancellation of the disturbance at **s**.

In practice **M** cannot be set exactly equal to **H**, but it can be made arbitrarily close (see below for implementation). Making **M** close to **H** has the effect of increasing stability in the system by making the magnitude of the term **G**(**M**-**H**) in the denominator less than 1. This guarantees that the Nyquist criterion for stability will be satisfied.

Also, in practice, **G** cannot always be chosen to be exactly equal to -1/**M**. In some cases **M** may not be minimum phase, which would require that **G** be acausal. However, by constructing **G** to equal -1/**M** over a small range of frequencies it is possible to achieve very good cancellation over a small band of frequencies of interest at the expense of poor cancellation at all other frequencies.

The control system described so far is very general. Before proceeding to the implementation for digital control systems, it is worth reviewing exactly what has and has not been accomplished. The decomposition of the controller into **G** and **M** cannot improve the overall performance of the control system.

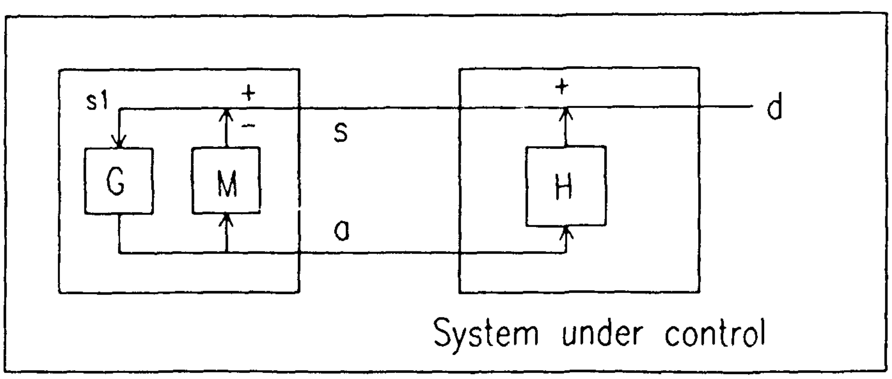

Figure 2 - control system decomposition

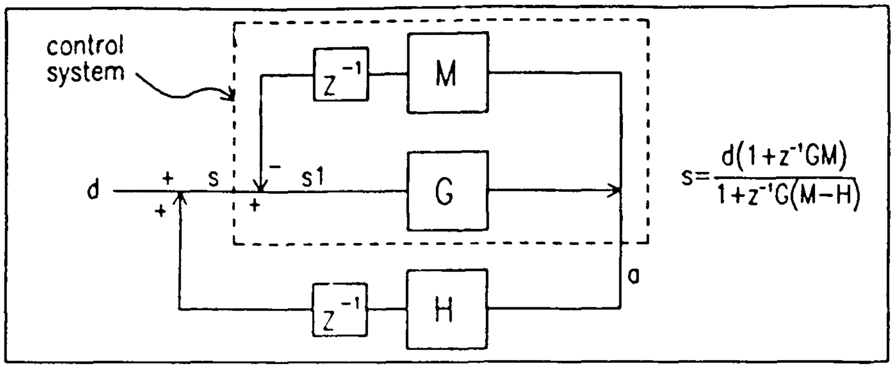

Figure 3 - digital control system with delays

That is, for a given **H**, noise level, signal ensemble, etc., the theoretical "best" controller performance remains the same when stated in terms of "greater than X dB cancellation of signals over a specified frequency range". What can be achieved, given the decomposition into **G** and **M**, is to determine **M** (the "modelling" aspect of the problem, which is easier than the "control" aspect) and, using **M**, then determine **G** using open-loop feedforward techniques. Future directions for adaptive implementation of the **M** and **G** functions will be discussed at the end of the paper.

DERIVATION OF THE MODEL AND CONTROL TRANSFER FUNCTIONS

We now proceed to show how the transfer functions **M** and **G** are derived for a digital control system. Figure 3 shows the system of Fig. 2 transformed into a more conventional closed-loop form. In addition, the **H** and **M** blocks of Fig. 2 have been decomposed further into new blocks concatenated with explicit sampling delays. The boundary of the control system is shown by a dotted line. For this discussion, the signal **s** is the digitized output of the control system's A/D converter (ADC) and signal **a** is the digital value to be sent to the system's D/A converter (DAC).

The program implemented in the control system is

1. Wait on clock for the next sample.
2. Read ADC and subtract the last model (**M**) output giving **s1**.
3. Apply **G** to **s1** giving **a** and send to DAC.
4. Apply **M** to **a** giving the next model output.

DERIVATION OF THE M TRANSFER FUNCTION

Because the digital controller in the loop is "smart" it is possible to inject a test signal into the system under control at the controller's output **a** and record the effect of the signal at the controller's input s. The set of pairs (x_i, y_i), where i = 0..N and the x's and y's are outputs to the actuator and inputs to the sensor respectively, then forms the basis for estimating **H**. Note that if a given **a** and **s** are paired during the same sample interval, then the resulting transfer function will include any sampling delays around the loop in addition to the external transfer function of the system under control.

The $\mathbf{M}$ transfer function is best realized in terms of an IIR (infinite impulse response) filter of the form

$$y_r = \sum_{k=0}^{m} b_k x_{r-k} + \sum_{k=1}^{n} a_k y_{r-k}. \tag{4}$$

This filter form includes both poles that will accurately model the mechanical or electrical response of $\mathbf{H}$ as well as zeroes that will model delays in $\mathbf{H}$. Many techniques are available for estimating $\mathbf{H}$ based on input and output data [2].

We chose to drive the actuator with a succession of sinusoids and analyze the response at the sensor using the single-line DFT

$$H(z) = \sum_{k=0}^{N-1} h_k\, z^{-k}, \quad \text{where } z = e^{j\omega T}, \tag{5}$$

to determine the complex amplitude response at equally spaced frequencies below the Nyquist limit. Using this method it is possible to achieve a high signal-to-noise ratio in the estimates of $\mathbf{H}$ as a function of frequency. The actual system transfer function obtained this way is multiplied by z to remove a one sample delay; the resulting transfer function corresponds to $\mathbf{H}$ in Fig. 3 above. The estimate of $\mathbf{M}$ is then computed by using the least-squares fit of $H(z_i)$ to an equation of the form

$$M(z) = \frac{\sum_{k=0}^{m} b_k z^{-k}}{1 - \sum_{k=1}^{n} a_k z^{-k}} \quad \text{or } M(z) = \frac{B(z)}{1 - A(z)}. \tag{6}$$

As a first approximation, the linear form of the equations

$$\left[\, 1 - A(z_i) \right] \cdot M(z_i) = B(z_i) \tag{7}$$

are fit setting $M(z_i)$ equal to the measured $H(z_i)$. The solution to this problem can then be used as a starting approximation for an iterative solution of Eq. (6) using the Levenburg-Marquadt or a similar technique.

Since Eq. (6) for $M(z)$ (with the a_k and b_k coefficients determine above) is analytic and assumed stable, it can be evaluated at any value of z on the unit circle.

In practice, the least-squares solution to Eq. (7) was an adequate approximation of $\mathbf{H}$.[1] Recalling Eq. (3), it is only necessary that $|\mathbf{M}-\mathbf{H}|$ be small for stability to be acceptable. For highly resonant systems, it may be necessary to fit Eq. (6) if noise in the system renders the first approximation unstable when implemented as an IIR filter.

DERIVATION OF THE G TRANSFER FUNCTION

Once $\mathbf{M}$ has been estimated, the construction of $\mathbf{G}$ such that $\mathbf{MG} \equiv -1$ over the frequency range of cancellation is theoretically straightforward.

First, it is necessary to choose a filter model for **G**. We chose the FIR (finite impulse response) filter model

$$G(z) = \sum_{k=0}^{m} g_k z^{-k} \tag{8}$$

because of its inherent stability. The construction of **G** then becomes a linear least-squares fit in the z domain using as "actual" values of $G(z_i)$

$$G(z_i) = -\frac{1}{M(z_i)} \tag{9}$$

at the appropriate z_i on the unit circle corresponding to the frequency range of interest.

It is important to use enough values z_i to overdetermine the problem. If, for example, the number of sample points on the unit circle is equal to the order of the FIR model, the solution will be exact for the frequencies specified, but may be poorly behaved even in the neighborhood of those frequencies. In practice, using roughly twice as many sample points as coefficients made the resulting FIR filters uniform in the region of interest.

EXPERIMENTAL INVESTIGATION

To investigate the above controller design, we first used a purely electrical system with no mechanical elements. Investigation of the design methodology on the mechanical system is still in progress. The electrical system consisted of

1. A summing op amp to implement the summing junction in Fig. 1.

2. An HP 35660A spectrum analyzer to generate the swept sinusoid disturbance **d** and to measure the signal **s** (the op amp's output) to verify the cancellation ability of the system.

3. A digital signal processor (ASPI's TMS32030-based product) and a 16 bit ADC and DAC module used to implement the digital control system. The sample rate of the control system was chosen as 125 kHz.

4. Software written by us to implement the **M** and **G** filters and to drive the output **a** during the determination of transfer function.
5. A cascaded low- and highpass filter pair (48 dB/octave) used to provide a realistic system transfer function **H**.

Consistent with the discussion above, the **H** of Fig. 2 consists of both the analog filters in the feedback loop and the digital delays in the ADC/DAC module. In fact, the time lag due to the I/O module alone is two sample times, arising from the buffered implementation of the ADC and DAC.

Figure 4 shows the amplitude response and group delay of the transfer function **H** from **a** to **s**.

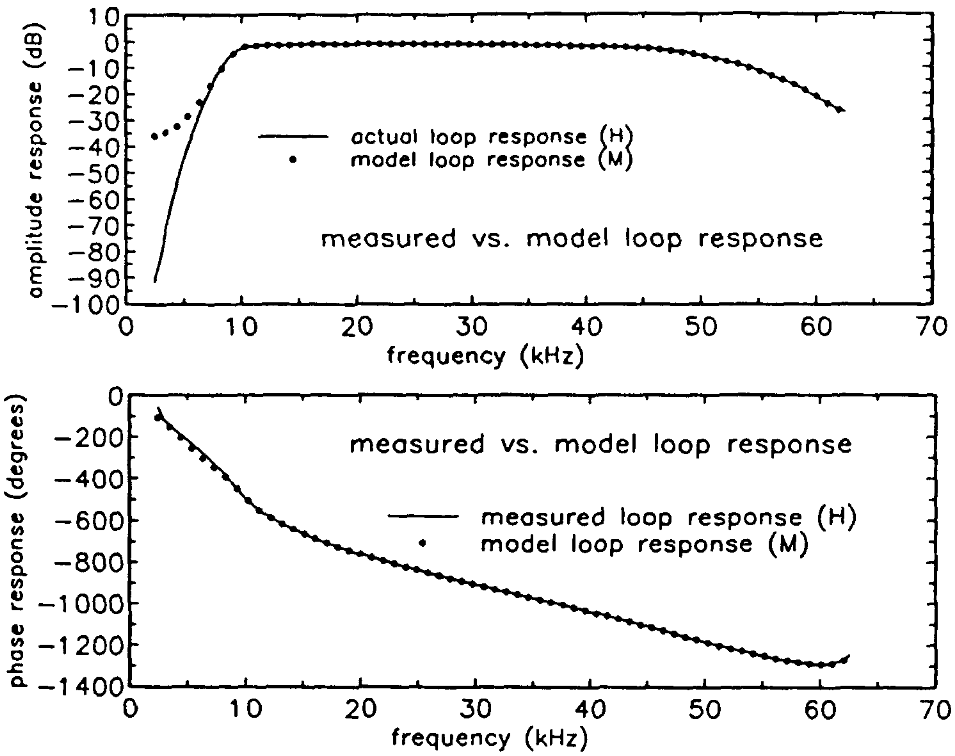

Figure 5 - actual vs. calculated response

DETERMINATION OF THE **M** TRANSFER FUNCTION

A filter order for **M** was chosen using m=9 and n=8 in Eq. (6) above. The comparison of **M** to the measured **H** is shown in Fig. 5. Note that the agreement of **M** and **H** is good except where |**H**| is small. The fit could be improved in this region by weighting the least-square design equations more heavily in the region below 10 kHz.

DETERMINATION OF THE **G** TRANSFER FUNCTION

A filter order of m=20 was chosen for the realization of **G** using Eq. (8). Forty equally spaced sample points, z_k, were chosen over each of the 4 kHz frequency ranges. A desired $G(z_k)$ was then calculated for each point using Eq. (9). These values were then fit to the FIR filter model in Eq. (8). As a check on stability, the term **G(M-H)** was plotted in the complex plane for all frequencies where **H** was measured. In all cases, the resulting path was entirely inside the unit circle with a maximum magnitude of |**G(M-H)**| equal to -6.8, -15, -18.5, and -20.3 dB (re unity) for the 10, 20, 30, and 40 kHz bands respectively. If the path had violated the Nyquist design criterion, it would have been necessary to either:

> improve the fit of **M** to **H** at the problem frequencies to reduce the difference |**M-H**|;

or

> place additional constraints on **G** in the least-squares fit by requiring that it be small at critical frequencies.

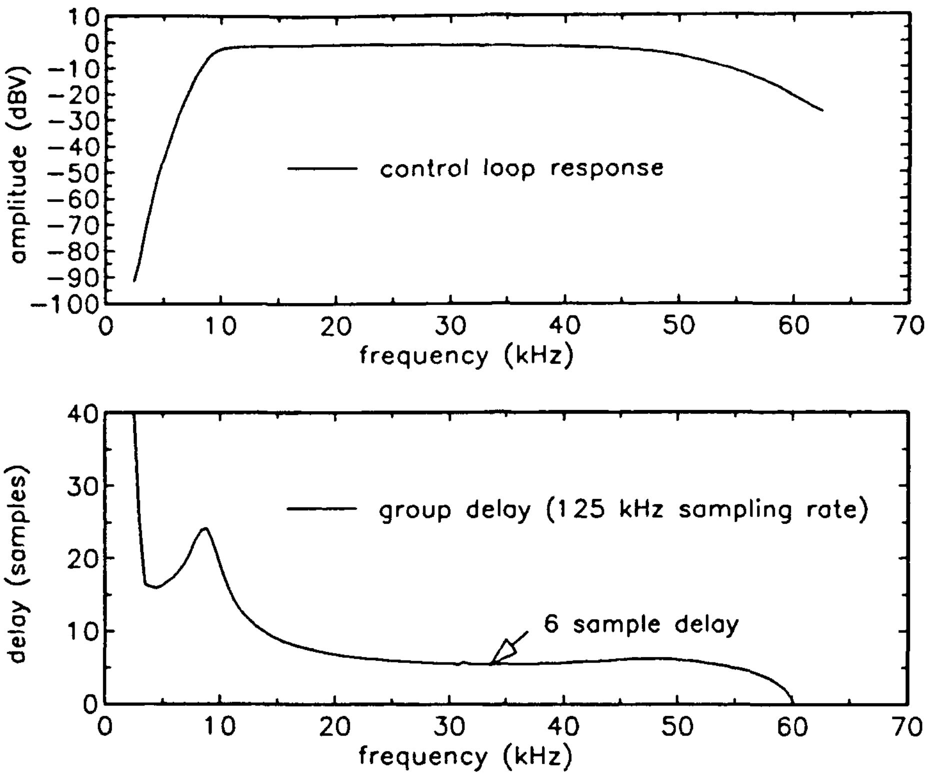

Figure 4 - measured control loop response

Note the large group delay of six samples or more in the system at virtually all frequencies. It is these large delays that make digital control difficult, since a delay of six samples produces a 180-degree phase shift every 10 kHz.

The design problem posed for this experiment was to construct four pairs of control functions G and M that would null the input s within a band 4 kHz wide starting at any one of four frequencies: 10, 20, 30, or 40 kHz.

Figure 6 shows the performance (20 log s/d) of the control systems designed for the specified frequencies. In all cases, the uncontrolled system has a flat magnitude response of unity (0 dB).

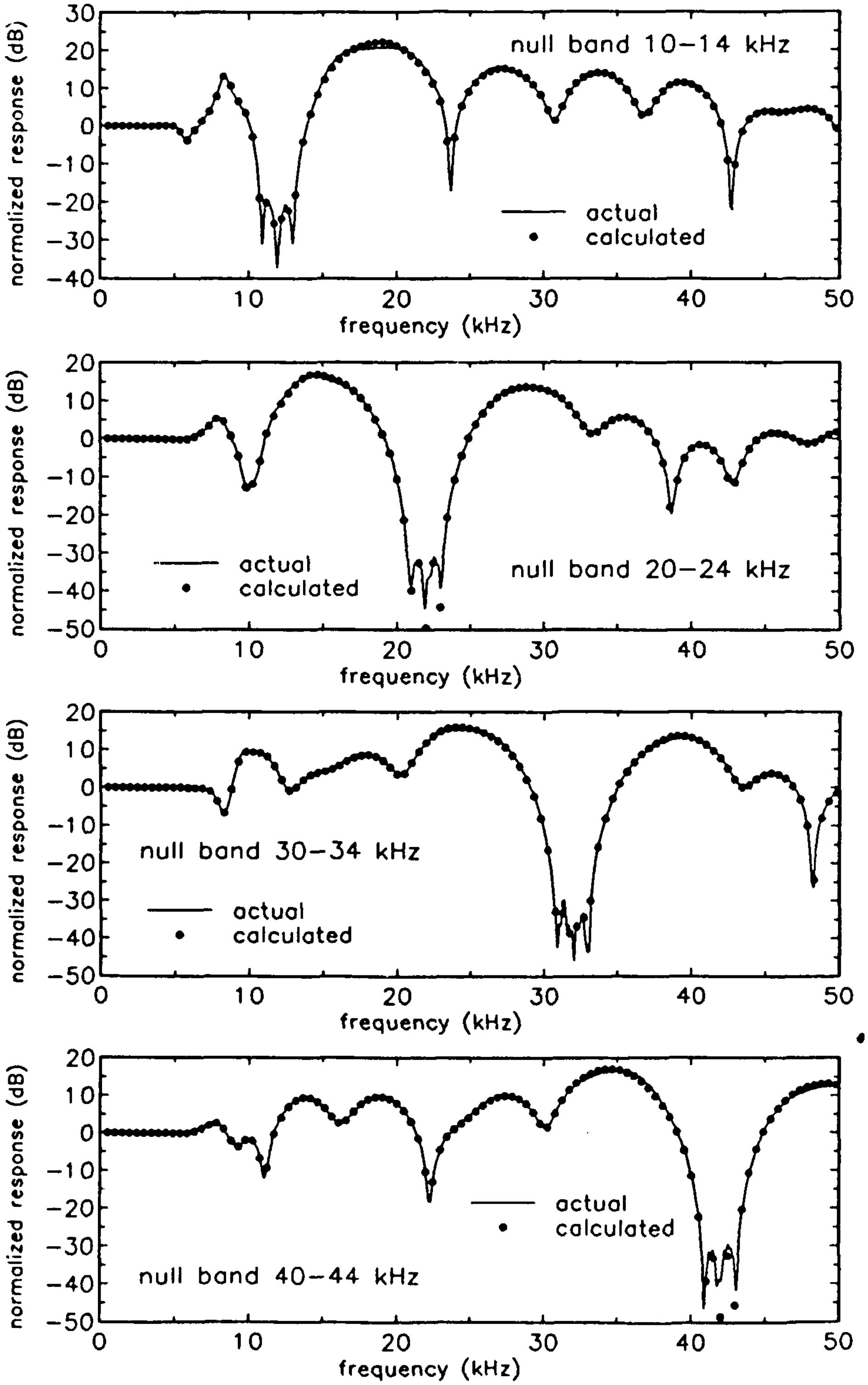

Figure 6 - performance of 10, 20, 30, and 40 kHz controllers

Four important qualitative results are evident from these plots:

1. Actual cancellation (roughly 30 dB in the center of the band) is uniform for the same filter design parameters, independent of which frequency range is chosen for cancellation. This is a good indication of the robustness of the design technique.

2. The agreement between the calculated controller performance and actual performance was excellent in all cases. This allows the designer to use simulation results with confidence.

3. Given the same design parameters, the cancellation achieved was poorest in the 10-14 kHz band. Of the four regions chosen, this is the region where the delays in **H** (Fig. 4) are largest, making the compensation problem more difficult.

4. In all cases, the cancellation in the band of interest was achieved at the expense of some <u>enhancement</u> in other parts of the spectrum. This unwanted enhancement can be controlled to some extent by varying the design parameters of the G filter, but the most serious limitation on performance is the cancellation bandwidth desired relative to delays in **H**.

FUTURE DIRECTIONS

Future work on this technique will lie in the area of determining **M** and **G** adaptively. The problem with adaptive implementation of feedback systems arises from the possibility that the adaptive filter may become unstable due to "noisy" nature of the adaptive path in coefficient space [3]. It is hoped that a good initial determination of **M** will provide increased stability to allow the adaptive implementation of **G**.

Future directions:

1. Currently, the estimate of **H** is made by driving **a** in absence of d, the external disturbance. For adaptive implementation of **M**, an algorithm must be specified that can estimate **H** even in the presence of d. Any desirable algorithm would bound the maximum allowable power that driving **a** would contribute at the summing point: test signals injected by the control system must be much "quieter" than the disturbance we are trying to control.

2. Can **M** and **G** be adapted simultaneously or should they be adapted alternately to help stability?

3. What is the best mix of computing time applied to adapting **M** and **G**?

CONCLUSIONS

Decomposing a feedback-based cancellation system into a model section **M** and a control section **G** offers a conceptual advantage when the control system to be designed has delays in the control loop. This conceptual advantage may result in real design advantages when the control system is to be implemented adaptively because of the increased decoupling of output to input offered by a good match of **M** to the actual control loop transfer function **H**.

References

1. M.D.McCollum, et al. 1991. "Electromechanical Modelling of an Active Isolation System" in Proceedings, Conference on Recent Advances in Active Control of Sound and Vibration, in preparation.

2. James H. McClellan. 1988. "Parametric Signal Modelling" in Advanced Topics in Signal Processing, Lim and Oppenheim, eds. Prentice Hall, pp. 1-58.

3. Widrow and Stearns. 1985. Adaptive Signal Processing, Prentice Hall, pp. 271-301.

4. Press, et al. 1986. Numerical Recipes, Cambridge University Press, pp. 52-60.

Footnotes

1. In solving all of the linear least-square systems described above, the Singular Value Decomposition (SVD) was used to overcome any near rank deficiencies in the L.S. design matrices [4]. In the least-squares formulation

$$A^tAx = A^tb,$$

the matrix A^tA was decomposed into $U\Sigma V$ and the inverse formed as

$$V^t\Sigma^{-1}U^t$$

with the elements of Σ^{-1} corresponding to $\sigma_i \leq 0.00001 \cdot \sigma_{max}$ in Σ set to 0.